Article

The Maximin Principle of □-Radical Packings

Thomas Devic, Min Yuan, Judy Adams, Daniel C. Fredrickson, Stephen Lee, and D. Venkataraman

J. Am. Chem. Soc., **2005**, 127 (42), 14616-14627• DOI: 10.1021/ja050346f • Publication Date (Web): 01 October 2005

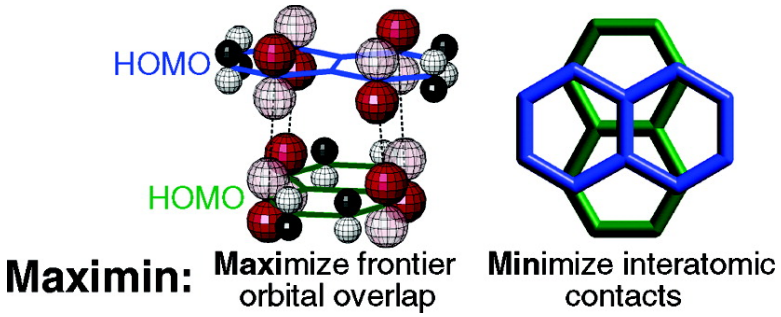

J|A|C|S
ARTICLES
Published on Web 10/01/2005

The Maximin Principle of π-Radical Packings

Thomas Devic,[†] Min Yuan,[†] Judy Adams,[†] Daniel C. Fredrickson,[†]
Stephen Lee,*[,†] and D. Venkataraman[‡]

Contribution from the Department of Chemistry and Chemical Biology, Baker Laboratory, Cornell University, Ithaca, New York 14853-1301, and Department of Chemistry, University of Massachusetts, Amherst, Massachusetts 01003

Received January 18, 2005; E-mail: sl137@cornell.edu

Abstract: A two-term model is proposed for hydrocarbon and N-containing π-radicals which are in close contact with one another. The first term is attractive (due to partially occupied frontier π-orbitals), and the second, repulsive (due to hard-core repulsion between close-lying atoms). This model is applied to dimers where intermolecular contacts are closer than $<0.95\times$ the sum of the atomic van der Waals radii. The maximin principle is proposed. The maximin principle states that the lowest energy conformation maximizes overlap of the frontier orbitals while *simultaneously* minimizing intermolecular contacts. A Hückel Hamiltonian, the μ_2-Hamiltonian, which contains the above attractive and repulsive terms, is applied. The interaction surfaces of two π-hydrocarbon radical cations were calculated for the three systems known crystallographically to contain cations in close contact: naphthalene, fluoranthene, and pyrene. The global minima of these surfaces correspond to the experimentally determined structures. The μ_2-Hamiltonian energy surfaces of the naphthalene cation dimer are qualitatively similar to those calculated at the RHF/6-311G(d,p) and MP2/6-311G(d,p) levels. The maximin principle is applied to N-containing π-radicals. Except in the case of tetracyanoethene, the maximin principle correctly predicts the most common dimer crystal packing. (MgPc)-(NO_3)·0.5THF and (MgPc)(ReO_4)·1.5THF (Pc = phthalocyanine) were prepared: both new crystal structures follow the maximin principle. The maximin principle is used to suggest the dimer cation ground state of oligoacenes, cations important as organic hole-based semiconductors.

1. Introduction

Our current understanding of π-system intermolecular interactions is somewhat perplexing. On one hand π-system reaction pathways are analyzed through their frontier orbitals, but on the other hand, the forces which control the crystal packing of these same molecules are often described by a purely electrostatic model. Thus, we have the Woodward−Hoffmann rules to govern π-system reaction pathways[1−8] but a purely quadrupole-quadrupole electrostatic coupling term to describe π (or $\pi-\sigma$) aromatic−aromatic interactions.[9−16]

In this paper we discuss π-systems where frontier orbitals model play a dominant role in crystal packing. We therefore investigate crystalline π-systems where C···C distances are short (C···C < 3.2 Å). This restriction to short C···C contacts largely limits our study to π-cations and anions. For these systems, π-frontier orbitals are known to play a significant role.[17−25] We and others[26,24] find this role can be more fully understood if interatomic repulsive energies are explicitly included. We propose a general crystal packing principle: the maximin principle. This principle states that the favored orientation of

[†] Cornell University.
[‡] University of Massachusetts.

(1) Woodward, R. B.; Hoffmann, R. *Angew. Chem., Int. Ed. Engl.* **1969**, *8*, 781−932.
(2) Baldwin, J. E.; Andrist, A. H.; Pinschmidt, R. K. *Acc. Chem. Res.* **1972**, *5*, 402−406.
(3) Berson, J. A. *Acc. Chem. Res.* **1972**, *5*, 406−414.
(4) Fleming, I. *Frontier Orbitals and Organic Chemical Reactions;* John Wiley & Sons: London, 1976.
(5) Lawless, M. K.; Wickham, S. D.; Mathies, R. A. *Acc. Chem. Res.* **1995**, *28*, 493−502.
(6) Kato, S. *Theor. Chem. Acc.* **2000**, *103*, 219−220.
(7) Williams, R. V. *Eur. J. Org. Chem.* **2001**, 227−235.
(8) Reyes, M. B.; Lobkovsky, E. B.; Carpenter, B. K. *J. Am. Chem. Soc.* **2002**, *124*, 641−651.
(9) Hashimoto, M.; Isobe, T. *Bull. Chem. Soc. Jpn.* **1972**, *45*, 299−300.
(10) Brown, N. M. D.; Swinton, F. L. *J. Chem. Soc., Chem. Commun.* **1974**, 770−771.
(11) Price, S. L.; Stone, A. J. *J. Chem. Phys.* **1987**, *86*, 2859−2868.
(12) Gavezzotti, A. *J. Am. Chem. Soc.* **1989**, *111*, 1835−1843.
(13) Hunter, C. A.; Sanders, J. K. *J. Am. Chem. Soc.* **1990**, *112*, 5525−5534.
(14) Hernández-Trujillo, J.; Costas, M.; Vela, A. *J. Chem. Soc., Faraday Trans.* **1993**, *89*, 2441−2443.
(15) Williams, D. E.; Xiao, Y. *Acta Crystallogr.* **1993**, *A49*, 1−10.
(16) Tsuzuki, S.; Honda, K.; Uchimaru, T.; Mikami, M.; Tanabe, K. *J. Am. Chem. Soc.* **2002**, *124*, 104−112.
(17) Awere, E. G.; Burford, N.; Haddon, R. C.; Parsons, S.; Passmore, J.; Waszczak, J. V.; White, P. S. *Inorg. Chem.* **1990**, *29*, 4821−4830.
(18) Michel, P.; Moradpour, A.; Penven, P.; Firlej, L.; Bernier, P.; Levy, B.; Ravy, S.; Zahab, A. *J. Am. Chem. Soc.* **1990**, *112*, 8285−8292.
(19) Kazmaier, P. M.; Hoffmann, R. *J. Am. Chem. Soc.* **1994**, *116*, 9684−9691.
(20) Almeida, M.; Henriques, R. T. *Handbook of Organic Conductive Molecules and Polymers;* John Wiley & Sons: 1997.
(21) Bryce, M. R.; Lay, A. K.; Chesney, A.; Batsanov, A. S.; Howard, J. A. K.; Buser, U.; Gerson, F.; Mersetter, P. *J. Chem. Soc., Perkin Trans. 2* **1999**, 755−764.
(22) Tyutyulkov, N.; Dietz, F.; Madjarova, G.; Müllen, K. *J. Phys. Chem. B* **2000**, *104*, 7320−7325.
(23) Takano, Y.; Taniguchi, T.; Isobe, H.; Kubo, T.; Morita, Y.; Yamamoto, K.; Nakasuji, K.; Takui, T.; Yamaguchi, K. *J. Am. Chem. Soc.* **2002**, *124*, 11122−11130.
(24) Small, D.; Zaitsev, V.; Jung, Y.; Rosokha, S. V.; Head-Gordon, M.; Kochi, J. K. *J. Am. Chem. Soc.* **2004**, *126*, 13850−13858.
(25) Geremia, S.; Costanzo, L. D.; Mardin, G.; Randaccio, L.; Purrello, R.; Sciotto, D.; Lauceri, R.; Pichierri, F. *Inorg. Chem.* **2004**, *43*, 7579−7581.
(26) Kamisuki, T.; Hirose, C. *Spectrochimica Acta A* **2000**, *56*, 2141−2148.

10.1021/ja050346f CCC: $30.25

interacting hydrocarbon or nitrogen containing π-systems is one which both maximizes HOMO−LUMO overlap and simultaneously minimizes interatomic contacts.

It proves possible to find a simple quantum mechanical model which incorporates both components of the maximin principle and whose standard predictions accord with observed experimental geometries. This model is the μ_2-Hückel Hamiltonian, a Hamiltonian dominated by both attractive frontier overlap interactions and repulsive interatomic nonbonding terms.[27] With this Hamiltonian, we generate intermolecular energy surfaces which agree both with known experimental crystal packings and with higher level ab initio calculations.[28−31] The numerical agreement between the μ_2-Hückel and ab initio Hartree−Fock surfaces, coupled with the fact that the μ_2-Hamiltonian is dominated by the frontier orbital and interatomic repulsion terms, confirms the underlying accuracy of the maximin principle. Hydrocarbon systems treated include all known π-systems with short C···C contacts: naphthalene,[32] fluoranthene,[33] and pyrene[34] cation dimers. These results suggest that both traditional electronic effects, such as frontier orbital mixing, and steric effects, such as hard sphere atomic repulsion, can be incorporated in the same simple tight-binding (or Hückel) Hamiltonian.

But the maximin principle is geometrically simple enough that it can be applied without actual dimer calculations. We show for a number of N-containing π-systems that, from a knowledge of the HOMO or LUMO alone, we can correctly predict the most common crystal packing. π-Systems considered include all those N-containing systems with short C···C, C···N, or N···CN contacts (distances $< 0.95 \times$ the sum of the van der Waals radii): phthalocyanine (2HPc),[35] metalated phthalocyanine (MPc),[36−38] metalated tetrabenzoporphyrin (MPp),[39−41] 1,2,3-tris(dicyanomethylene)cyclopropane (HCCP),[42,43] 7,7,8,8-tetra-cyanoquinodimethane (TCNQ),[44−65] *N*,*N*′-dicyano-1,4-benzoquinodiimine (DCNQI),[66] 1,1,2,5,6,6-hexacyano-3,4-diazahexadiene (BTCQ),[67] and tetracyanoethene (TCNE).[68−75] (See Supporting Information for CSD search results.) We further prepare two new phthalocyanine based cation radical salts which further verify the utility of the maximin principle.

2. Technical Procedures

2.1. Introduction to the μ_2-Hückel Method. Before explicitly stating the equations used in μ_2-Hückel calculations, some further introductory statements about π-system intermolecular interactions are helpful. We begin by noting that frontier orbital pictures have not proven very useful in accounting for π-system packing interactions.[9−16] Instead, the two commonly observed aromatic packing motifs, both the staggered $\pi-\pi$ stacking and the herringbone pattern of pairs of aromatic rings, are generally viewed as two different minima of the quadrupole−quadrupole electrostatic interaction surface.

The small role frontier orbitals play in these packings can be understood qualitatively. The leading term in frontier orbital interactions is proportional to $S^2/\Delta E$, where S and ΔE refer to respectively the orbital overlap and the difference in energy between the HOMO and LUMO.[4] In neutral aromatic systems, the C···C intermolecular distances are long and the HOMO−LUMO energy gap is large. The numerator and the denominator of the frontier orbital interaction term are, respectively, small and large; the overall frontier orbital interaction is tiny.

In this paper by contrast we consider a very different set of π-systems. We consider π-cations and anions with C···C intermolecular interactions less than 3.2 Å. Such cations and anions have partially filled HOMOs and LUMOs, and as the interatomic distances are short, overlaps are large. The two contrasting cases are shown in Figure 1. It is not suprising that frontier orbital interactions are small for the former systems but large for the latter ones.

At the same time, it is evident that the maximization of π-overlap is not by itself sufficient to account for the observed geometries of interacting π-systems. Were maximization of π-overlap alone the governing principle behind intermolecular interactions, the preferred orientation of neighboring π-systems would be a fully eclipsed one, with one π-system directly on top of a similarly oriented second molecule. Such an eclipsed stacking would necessarily maximize

(27) Pettifor, D. *Bonding and Structure of Molecules and Solids;* Clarendon Press: Oxford, 1995.
(28) Lee, S.; Foran, B. *J. Am. Chem. Soc.* **1994**, *116*, 154−161.
(29) Rousseau, R.; Lee, S. *J. Chem. Phys.* **1994**, *101*, 10753−10765.
(30) Tse, J. S.; Frapper, G.; Ker, A.; Rousseau, R.; Klug, D. D. *Phys. Rev. Lett.* **1999**, *82*, 4472−4475.
(31) Ker, A.; Todorov, E.; Rousseau, R.; Uehara, K.; Lannuzel, F.-X.; Tse, J. S. *Chem.−Eur. J.* **2002**, *8*, 2787−2798.
(32) Fritz, H. P.; Gebauer, H.; Friedrich, P.; Ecker, P.; Artes, R.; Schubert, U. *Z. Naturforsch.* **1978**, *33b*, 498−506.
(33) Enkelmann, V.; Morra, B. S.; Kröhnke, C.; Wegner, G.; Heinze, J. *Chem. Phys.* **1982**, *66*, 303−313.
(34) Lee, S.; Chen, B.; Fredrickson, D. C.; DiSalvo, F. J.; Lobkovsky, E.; Adams, J. A. *Chem. Mater.* **2003**, *15*, 1420−1433.
(35) Gardberg, A. S.; Sprauve, A. E.; Ibers, J. A. *Inorg. Chim. Acta* **2002**, *328*, 179−184.
(36) Martinsen, J.; Stanton, J. L.; Greene, R. L.; Tanaka, J.; Hoffman, B. M.; Ibers, J. A. *J. Am. Chem. Soc.* **1985**, *107*, 6915−6920.
(37) Yakushi, K.; Yamakado, H.; Yoshitake, M.; Kosugi, N.; Kuroda, H.; Sugano, T.; Kinoshita, M.; Kawamoto, A.; Tanaka, J. *Bull. Chem. Soc. Jpn.* **1989**, *62*, 687−696.
(38) Gardberg, A. S.; Deng, K.; Ellis, D. E.; Ibers, J. A. *J. Am. Chem. Soc.* **2002**, *124*, 5476−5480.
(39) Yakushi, K.; Yoshitake, M.; Kuroda, H.; Kawamoto, A.; Tanaka, J.; Sugano, T.; Kinoshita, M. *Bull. Chem. Soc. Jpn.* **1988**, *61*, 1571−1576.
(40) Barkigia, K. M.; Renner, M. W.; Fajer, J. *J. Phys. Chem. B* **1997**, *101*, 8398−8401.
(41) Vangberg, T.; Lie, R.; Ghosh, A. *J. Am. Chem. Soc.* **2002**, *124*, 8122−8130.
(42) Ward, M. D.; Fagan, P. J.; Calabrese, J. C.; Johnson, D. C. *J. Am. Chem. Soc.* **1989**, *111*, 1719−1732.
(43) Miller, J. S.; Ward, M. D.; Zhang, J. H.; Reiff, W. M. *Inorg. Chem.* **1990**, *29*, 4063−4072.
(44) Fritchie, C. J.; Arthur, P. *Acta Crystallogr.* **1966**, *B21*, 139−145.
(45) Goldberg, S. Z.; Eisenberg, R.; Miller, J. S.; Epstein, A. J. *J. Am. Chem. Soc.* **1976**, *98*, 5173−5182.
(46) Schultz, A. J.; Stucky, G. D.; Blessing, R. H.; Coppens, P. *J. Am. Chem. Soc.* **1976**, *98*, 3194−3201.
(47) van der Wal, R. J.; van Bodegom, B. *Acta Crystallogr.* **1978**, *B34*, 1700−1702.
(48) Lau, C.-P.; Singh, P.; Cline, S. J.; Seiders, R.; Brookhart, M.; Marsh, W. E.; Hodgson, D. J.; Hatfield, W. E. *Inorg. Chem.* **1982**, *21*, 208−212.
(49) Endres, H. *Angew. Chem., Int. Ed. Engl.* **1984**, *23*, 999−1000.
(50) Middeldorp, J. A. M.; Visser, R. J. J.; de Boer, J. L. *Acta Crystallogr.* **1985**, *B41*, 369−374.
(51) Bryce, M. R.; Moore, A. J.; Bates, P. A.; Hursthouse, M. B.; Liu, Z.-X.; Nowak, M. J. *Chem. Commun.* **1988**, 1441−1442.
(52) Bencini, A.; Midollini, S.; Zanchini, C. *Inorg. Chem.* **1989**, *28*, 1963−1969.
(53) Fedin, V. P.; Sokolov, M. N.; Virovets, A. V.; Podberezskaya, N. V.; Fedorov, V. Y. *Inorg. Chim. Acta* **1992**, *194*, 195−200.
(54) Cornelissen, J. P.; van Diemen, J. H.; Groeneveld, L. R.; Haasnoot, J. G.; Spek, A. L.; Reedijk, J. *Inorg. Chem.* **1992**, *31*, 198−202.
(55) Oshio, H.; Ino, E.; Mogi, I.; Ito, T. *Inorg. Chem.* **1993**, *32*, 5697−5703.
(56) Dolbecq, A.; Fourmigué, M.; Batail, P.; Coulon, C. *Chem. Mater.* **1994**, *6*, 1413−1418.
(57) Aqad, E.; Becker, J. Y.; Bernstein, J.; Ellern, A.; Khodorkovsky, V.; Shapiro, L. *Chem. Commun.* **1994**, 2775−2776.
(58) Malatesta, V.; Millini, R.; Montanari, L. *J. Am. Chem. Soc.* **1995**, *117*, 6258−6264.
(59) Muñoz, M. C. *Acta Crystallogr.* **1995**, *C51*, 873−876.
(60) Fourmigué, M.; Perrocheau, V.; Clérac, R.; Coulon, C. *J. Mater. Chem.* **1997**, *7*, 2235−2241.
(61) Brook, D. J. R.; Koch, T. H. *J. Mater. Chem.* **1997**, *7*, 2381−2385.
(62) Ballester, L.; Gil, A. M.; Gutiérrez, A.; Perpiñán, M. F.; Azcondo, M. T.; Sánchez, A. E.; Amador, U.; Campo, J.; Palacio, F. *Inorg. Chem.* **1997**, *36*, 5291−5298.
(63) Fortin, D.; Drouin, M.; Harvey, P. D. *Inorg. Chem.* **2000**, *39*, 2758−2769.
(64) Choi, H. J.; Suh, M. P. *Inorg. Chem.* **2003**, *42*, 1151−1157.
(65) Zhao, H.; Bazile, M. J.; Galán-Mascarós, J. R.; Dunbar, K. R. *Angew. Chem., Int. Ed.* **2003**, *42*, 1015−1018.
(66) Aumüller, A.; Erk, P.; Hünig, S.; von Schütz, J. U.; Werner, H.-P.; Wolf, H. C.; Klebe, G. *Chem. Ber.* **1991**, *124*, 1445−1451.
(67) Decoster, M.; Conan, F.; Kubicki, M.; Le Mest, Y.; Richard, P.; Sala Pala, J.; Toupet, L. *J. Chem. Soc., Perkin Trans. 2* **1997**, 265−271.

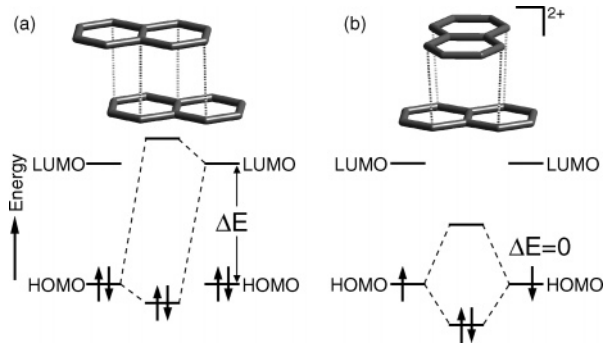

Figure 1. Frontier orbital interactions in neutral naphthalene and cationic naphthalene species. In neutral molecules, intermolecular distances are long and the frontier orbital overlaps are small. In the cationic molecules, intermolecular distances are short and frontier orbital overlaps are large.

HOMO−HOMO contact of a partially filled HOMO. But, except in some of the simpler π-systems,[68−75] such fully eclipsed geometries are not seen.

This can be understood if we consider the C···C interatomic potential. As is well-known, such interatomic potentials have a short-range highly repulsive component coupled with longer range attractive terms.[76,77] The repulsive component dominates the interaction energy at distances shorter than the sum of the van der Waals radii of the pair of interatomic atoms. In the case of carbon, with a van der Waals radius of 1.70 Å, this sum is 3.40 Å. The interaction energy minimum occurs to the right of this sum, near 3.80 Å for carbon.

In this paper we are interested in π-systems where the shortest C···C distances are less than 3.2 Å, a number significantly less than 3.40 Å. As the molecules are planar, and as the lowest energy geometries involve molecules where these planes are face-to-face, all close neighboring atoms are perforce at the same short C···C distance. In Figure 2, we draw a generic diagram of the C···C interatomic potential (from empirical C···C interaction energy parameters[78]). As this figure shows, such close C···C distances are in a highly repulsive regime of the interatomic potential. Figures 1 and 2 present the two portions of the maximin principle. We wish to optimize the HOMO−LUMO interaction between neighboring molecules (Figure 1) while minimizing the number of interatomic contacts (Figure 2). In the next section, we give the specific equations which incorporate the two effects.

2.2. μ_2-Hückel Calculations. In the μ_2-Hückel method used in this paper,[27,79] the total energy E_T is expressed by

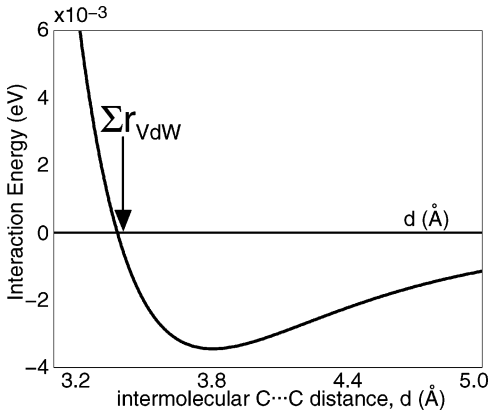

Figure 2. A qualitative diagram of the C···C interatomic potential plotting interaction energy vs intermolecular C···C distance. The interaction energy minumum lies near d = sum of the atomic two carbon van der Waals radii (3.4 Å).

$$E_T = U(r) - V(r) \quad (1)$$

where $U(r)$ is a hard-core interatomic repulsion energy, $V(r)$ is an attractive bonding energy, and r is a parameter dependent on the size of the system. In our case, the repulsive energy is roughly proportional to the number of intermolecular contacts and the attractive energy is dominated by frontier orbital interactions. The total energy E_T is given as

$$E_T = \gamma \int_{-\infty}^{\infty} (E - E_{ave})^2 \rho(E, r)\, dE + \int_{-\infty}^{E_F} E\rho(E, r)\, dE \quad (2)$$

where the above integrals represent the repulsive and the attractive energies, respectively. Here $\rho(E, r)$ is the electronic density of the valence bands, E_F is the Fermi energy, E_{ave} is the average energy of the electronic density of states, and γ is a proportionality constant. The density $\rho(E, r)$ is found from the diagonalization of the Hamiltonian matrix. As has been discussed elsewhere, the above repulsive and attractive energies are controlled by, respectively, the number of intermolecular contacts and the frontier orbital interactions.

Rather than explicitly calculating γ, we use the second moment scaling approximation.[27,79] Following the literature, the difference in energy between two structures A and B is approximately

$$E_T(A) - E_T(B) = \int_{-\infty}^{\infty} E\rho_A(E, r_{expt})\, dE - \int_{-\infty}^{E_F} E\rho_B(E, r_{scaled})\, dE \quad (3)$$

where the size of the B system has been scaled so that

$$\int_{-\infty}^{\infty} (E - E_{ave})^2 \rho_A(E, r_{expt})\, dE = \int_{-\infty}^{\infty} (E - E_{ave})^2 \rho_B(E, r_{scaled})\, dE \quad (4)$$

As eqs 2 and 3 imply, under such scaling conditions, the repulsive energy cancels and the difference in energy between the two structures is the difference in the attractive energies.

Diagonal elements, H_{ii}, are set equal to prescribed Coulombic integral values, while off-diagonal elements are based on the Wolfsberg−Helmholz approximation, $H_{ij} = {}^1/_2 KS_{ij}(H_{ii} + H_{jj})$.[80] The parameter K is set to 1.75, and orbitals are assumed to be single-ζ Slater type orbitals. We use the standard extended Hückel parameters for both carbon and hydrogen. The carbon parameters are loosely based on atomic Hartree−Fock calculations. The parameters for the carbon atoms are $H_{ii}(2s) = -21.40$ eV, $H_{ii}(2p) = -11.40$ eV; $\zeta(2s) = \zeta(2p) = 1.625$, while for the hydrogen atoms they are $H_{ii}(1s) = -13.60$ eV and $\zeta(1s) = 1.30$.[81]

(68) Lemenovskii, D. A.; Stukan, R. A.; Tarasevich, B. N.; Slovokhotov, T. L.; Antipin, M. Y.; Kalinin, A. E.; Struchkov, Y. T. *Koord. Khim.* **1981**, *7*, 240−249.
(69) Miller, J. S.; O'Hare, D. M.; Chakraborty, A.; Epstein, A. J. *J. Am. Chem. Soc.* **1989**, *111*, 7853−7860.
(70) Bock, H.; Ruppert, K.; Fenske, D.; Goesmann, H. *Z. Anorg. Allg. Chem.* **1991**, *595*, 275−284.
(71) Olmstead, M. M.; Speier, G.; Szabó, L. *J. Chem. Soc., Chem. Commun.* **1994**, 541−543.
(72) Johnson, M. T.; Campana, C. F.; Foxman, B. M.; Desmarais, W.; Vela, M. J.; Miller, J. S. *Chem.—Eur. J.* **2000**, *6*, 1805−1810.
(73) Del Sesto, R. E.; Sommer, R. D.; Miller, J. S. *CrystEngComm* **2001**, *47*, 1−3.
(74) Lü, J.-M.; Rosokha, S. V.; Kochi, J. K. *J. Am. Chem. Soc.* **2003**, *125*, 12161−12171.
(75) Jung, Y.; Head-Gordon, M. *Phys. Chem. Chem. Phys.* **2004**, *6*, 2008−2011.
(76) Heine, V.; Robertson, I. J.; Payne, M. C. *Bonding and Structure of Solids;* Haydock, R.; Inglesfield, J. E.; Pendry, J. B., Eds.; Royal Society: London, 1991.
(77) Stone, A. J. *The Theory of Intermolecular Forces;* Clarendon Press: Oxford, 1996.
(78) Mirsky, K. The determination of the intermolecular interaction energy by empirical methods. In *Computing in Crystallography: Proceedings of an International Summer School on Crystallographic Computing Held in Twente, The Netherlands 24 July-1 August, 1978*; Schenk, H., Olthof-Hazekamp, R., Koningsveld, H. V., Eds.; Delft University Press: Delft, 1978.
(79) Lee, S. *Annu. Rev. Phys. Chem.* **1996**, *47*, 397−419.
(80) Wolfsberg, M.; Helmholz, L. *J. Chem. Phys.* **1952**, *20*, 837−843.
(81) Hoffmann, R. *J. Chem. Phys.* **1963**, *39*, 1397−1412.

2.3. Ab Initio Calculations. Electronic structure calculations were performed for the neutral structures of naphthalene, fluoranthene, pyrene, H_2Pc, MgPc, MgPp, HCCP, TCNQ, DCNQI, BTCQ, DCNQI, and TCNE using the *Gaussian 98* software.[82] These structures were optimized at the Restricted Hartree−Fock level with the 6-31G(d) basis set. Pictures of the frontier orbitals for the resulting geometries were generated using the Molden program.

Calculations on the naphthalene$^+$ dimer were also carried out. Two naphthalene molecules (in the RHF-optimized structure described in the previous paragraph) were placed in 308 symmetrically distinct conformations (based on a 14 × 28 grid) in $\pi-\pi$ contact with an interplanar spacing of 3.2 Å. Single-point calculations were carried out on each conformation, with a 2+ charge for the dimer and a singlet spin state, at the RHF/6-311G(d,p) and MP2/6-311G(d,p) levels.[83] The magnitude of the basis set superposition error (BSSE) was checked using the counterpoise method at the minimum energy geometry.[84] For the RHF surface, the BSSE energy was 0.08 eV, small compared to the energetic variations between dimer conformations (0.37−1.20 eV). The BSSE energy was larger for the MP2 calculations (0.24 eV), so a correction was added to the calculated MP2 energies interpolated from a 4 × 8 grid of BSSE calculations.

2.4. Electrocrystallization of Phthalocyanine Salts. Magnesium(II) phthalocyanine (MgPc) was purchased from Strem Chemicals and was purified by sublimation at 400 °C twice prior to use. Crystals of **1** (MgPc)(NO_3)·0.5THF and **2** (MgPc)(ReO_4)·1.5THF were grown by applying anodic constant current, respectively, at $I = 4$ and 2 μA using platinum wire electrodes ($l = 2$ cm, $d = 0.8$ mm) and a two-compartment electrocrystallization cell. The electrolyte support was a solution of either 63 mg of (n-Bu_4N)NO_3 (for **1**) or 68 mg of (n-Bu_4N)-ReO_4 (for **2**) dissolved in 10 mL of freshly distilled tetrahydrofuran (THF). MgPc (8 and 6.5 mg for **1** and **2**, respectively) was dissolved in the anodic compartment. Black air-sensitive crystals suitable for X-ray diffraction were harvested after 5 days at −5 °C for **1** and 12 days at 20 °C for **2**.

2.5. CSD Search Parameters. Our Cambridge Structural Database (CSD) search on π-hydrocarbon radicals assumed intermolecular C···C distances between 2.50 and 3.25 Å (CSD version 5.25, which contains structures through Nov. 2003). Only organic structures with 3D coordinates were considered. As we were interested in π-hydrocarbon structures, N, Si, O, and S elements were excluded. All systems containing sp^3 carbon atoms were excluded. Fullerene molecules were excluded. We manually verified that the resultant structures involved ionic radical species. The search uncovered only two structures: (naphthalene)$_2PF_6$ (CSD codes: *naphtp01*, *naphtp10*)[32,85] and (fluoranthene)$_2AsF_6$ (*bosjuo*).[33] We added to this search the structure of (pyrene)$_{10}(I_3)_4(I_2)_{10}$, a crystalline compound which we have recently prepared and which meets the above criteria.[34]

The same procedure was adopted in our N-containing π-radical search except, of course, we allowed the presence of nitrogen atoms. The resulting data can be split in two groups: phthalocyanine (Pc) or related macrocycles, H_2Pc,[35] MPc,[36−38] and MPp[39−41] (we kept those Pc molecules coordinated to metal atoms, M), and nitrile derivatives, HCCP,[42,43] TCNQ,[44−65] DCNQI,[66] BTCQ,[67] and TCNE.[68−75] (See Supporting Information for CSD search results. Due to the large number of hits on TCNQ, only part of the TCNQ references are given here.) We added to the database two magnesium(II) phthalocyanine radical cation salts which we have electrochemically synthesized and structurally characterized (see both above and Supporting Information). For TCNQ−metal complexes, systems where the short contact was due to a hydrogen bond were manually removed.

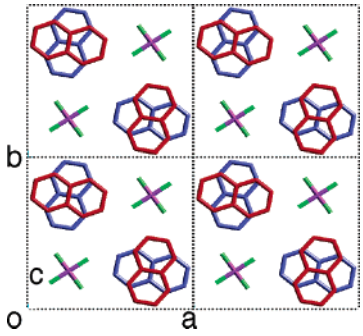

Figure 3. Crystal structure of (naphthalene)$_2PF_6$. C, red and blue; P, purple; F, green. Note the 90° rotation between the stacked naphthalene moieties in red and blue.

3. Results

3.1. Oxidized Hydrocarbon π-Systems. 3.1.1. Naphthalene Cations. Only a single crystalline compound of naphthalene cation radicals with short C···C distances (C···C = 3.20 Å) is known: (naphthalene)$_2PF_6$.[32,85] Its structure has been determined at both low temperature (123 K) and at room temperature. Both crystal structure determinations are similar and are based on stacks of naphthalene radicals. Within each stack, neighboring naphthalene molecular rings are rotated by 90° with respect to each other, giving the naphthalene stacks an alternating appearance. The closest C···C contacts are at 3.20−3.21 Å between carbon atoms at the 1, 4, 5, and 8 positions (see Figure 6 for ring numbering schemes) of neighboring naphthalene molecules; see Figure 3.

We compare this structure with model calculations on two naphthalene cations. In Figure 4, we plot the μ_2-Hückel energy for a pair of naphthalene cations. As in this article we are interested in face-to-face orientations of the π-systems, we consider only geometries in which these planes are parallel with each other at the fixed distance of 3.2 Å. Under such a restriction, the geometry of two naphthalene molecules reduces to just three variables: the displacement of the center-of-mass of the two molecules and the different orientation of the two molecules. As Figure 5 shows, these three parameters can be expressed as the three variables: x, y, and θ.

The electronic surface is presented as a contour map where red and blue correspond, respectively, to low and high energy. In Figure 4, the contour map as a function of x and y are presented for four different values of θ: 0°, 30°, 60°, and 90°. As this figure shows, the principal minima are found at (x, y) = (0, 0). The global minimum is at these values with $\theta = 90°$. This global minimum is 0.22 eV lower in energy than the fully eclipsed configuration ($\theta = 0°$). This theoretical minimum is the one observed experimentally.

The global minimum structure can be understood through knowledge of the HOMO π-orbital and the maximin principle. This HOMO is shown in Figure 6 at both the Hückel and RHF/6-31G(d) levels. As these calculations show, the HOMO has a strong presence at the 1, 4, 5, and 8 sites, a smaller presence at

(82) Frisch, M. J. et al. *Gaussian 98*, revision A.9; Gaussian Inc.: Pittsburgh, PA, 1998.
(83) The problem of the most quantitatively accurate method of calculation of intramolecular energy goes beyond the realm of this paper. It has recently been shown that to calculate ab initio intermolecular energies, the highest level of theory can be required. Our purpose here is to show that a simple Hückel method bears features in common with experimental structural data and also with good but not the highest level of ab initio calculations. See (a) Sinnokrot, M. O.; Valeev, E. F.; Sherrill, C. D. *J. Am. Chem. Soc.* **2002**, *124*, 10887−10893. (b) Sinnokrot, M. O.; Sherrill, C. D. *J. Am. Chem. Soc.* **2004**, *126*, 7690−7697. (c) Sinnokrot, M. O.; Sherrill, C. D. *J. Phys. Chem. A* **2004**, *108*, 10200−10207. (d) Heβelmann, A.; Jansen, G.; Schütz, M. *J. Chem. Phys.* **2005**, *122*, 014103.
(84) Boys, S. F.; Bernardi, F. *Mol. Phys.* **1970**, *19*, 553−566.
(85) Le Maguerès, P.; Lindeman, S. V.; Kochi, J. K. *Org. Lett.* **2000**, *2*, 3567−3570.

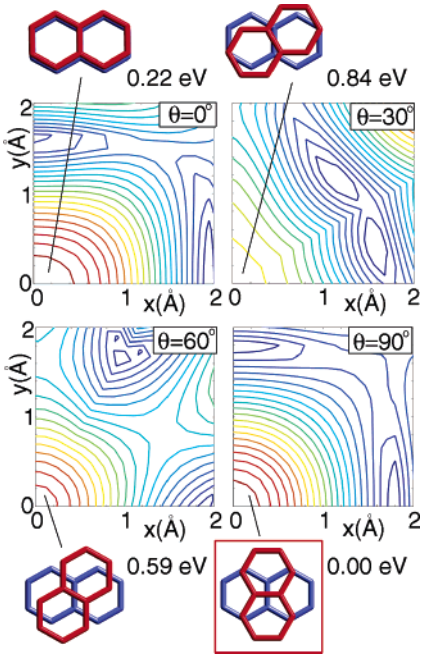

Figure 4. Contour maps of μ_2-Hückel calculations showing the variation of energy of $(naphthalene)_2^{2+}$ dimer with respect to its geometry (higher energy areas in blue and lower in red). See Figure 5 for definitions of *x*, *y*, and θ. The global energy minimum geometry is shown in red box.

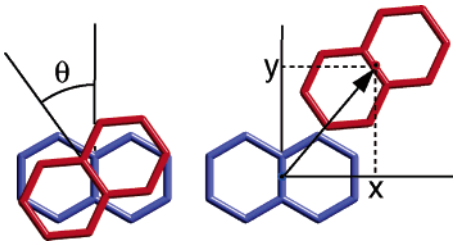

Figure 5. The three parameters used in the energy contour map: *x*, *y*, and θ. *x* and *y*: the relative position of the center-of-mass of the naphthalene moieties. θ: naphthalene rotation angle.

the 2, 3, 6, and 7 sites, and (by symmetry) no presence at the 8a or 4a positions. The maximin principle suggests that we would like to have contacts between the adjacent 1, 4, 5, and 8 positions while at the same time minimizing contacts between all remaining positions. The most favorable way of meeting these conditions is by stacking naphthalene rings directly on top of one another with a 90° rotation to one of the molecules.

We may compare the μ_2-Hückel energies to those from higher level ab initio calculations. In Figure 7 we plot higher level electronic surfaces (calculated with the RHF and MP2 methods) using the same *x*, *y*, and θ variables considered previously. A comparison of Figures 4 and 7 show great similarity between the two surfaces. In both cases there is a minimum for $(x, y) = (0, 0)$ and a ring of high energy structures in an approximate circle for (x, y) values roughly 1.5 Å away from this minimum. (Ab initio calculations were also conducted for $(naphthalene)_2^{2+}$ dimer at $x = y = 0$, $\theta = 0°$ conformation and compared to the $x = y = 0$, $\theta = 90°$ conformation. The 0° geometry was found to be 0.40 and 0.20 eV higher in energy than the 90° geometry at the HF and the MP2 levels, respectively.) The μ_2-Hückel energy (0.22 eV) is in good agreement with the MP2 level calculations.

In comparing theoretical to experimental results, we have so far compared somewhat different cases. The experimental

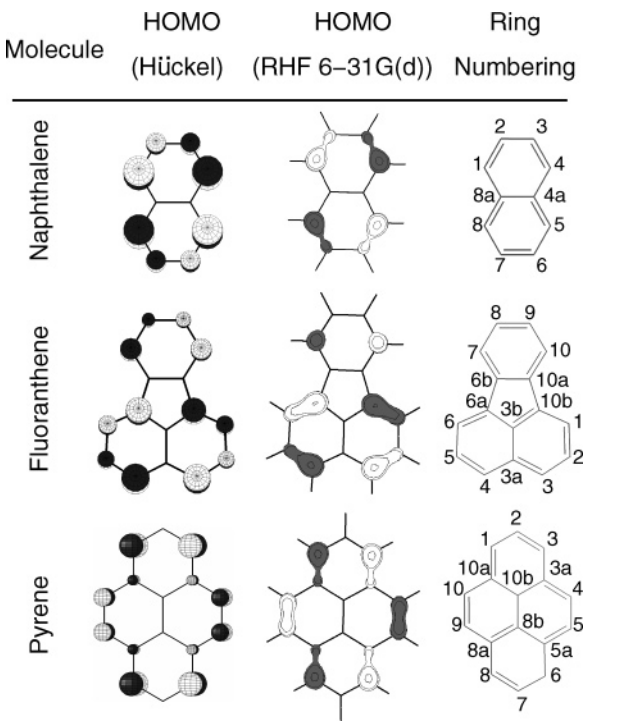

Figure 6. HOMO orbital configurations of naphthalene, fluoranthene, and pyrene moieties at both the Hückel and RHF/6-31G(d) levels. Canonical ring numbering of these molecules are also shown on the right column.

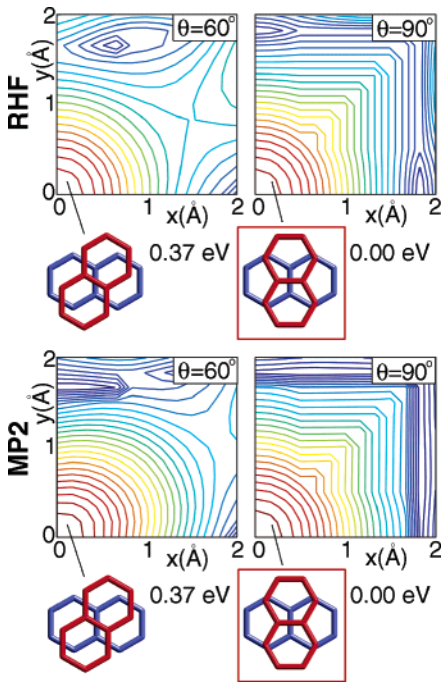

Figure 7. Contour maps of ab initio energies (top, RHF; bottom, MP2) calculated for the $(naphthalene)_2^{2+}$ dimer (interplanar spacing of 3.2 Å, basis set 6-311G(d,p)). See Figure 5 for definitions of *x*, *y*, and θ and Figure 4 for color conventions.

system involves a dimer cation with a total single positive charge. Both the μ_2-Hückel and ab initio results were for a dimer cation with an overall plus two charge. We can compare these experimental vs theoretical cases as they are related. As Figure 1 suggests, in the case of $(naphthalene)_2^{+2}$, the intermolecular bonding HOMO orbital is completely occupied and the intermolecular antibonding LUMO is empty. By contrast, in the single positive charge dimer, there is one additional electron in

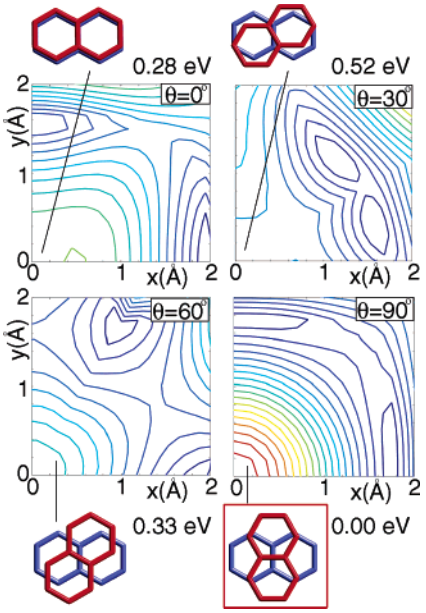

Figure 8. Contour maps of μ_2-Hückel calculations showing the variation of energy of $(\text{naphthalene})_2^{1+}$ dimer with respect to its geometry (higher energy areas in blue and lower in red). See Figure 5 for definitions of x, y, and θ. The global energy minimum geometry is shown in red box.

the antibonding orbital. This antibonding term will reduce roughly half the attractive potential found in the +2 system. The monocharged dimer electronic surface is shown in Figure 8. As a comparison of Figures 4 and 8 shows, it resembles the dication surface, but where the attractive potential is decreased roughly by a factor of 2. This antibonding term is more pronounced in the case where there are more intermolecular contacts i.e., $\theta = 0°$, resulting in a higher energy surface.

As the interest of our paper is in the minima due to frontier orbital interactions, it is worthwhile to pay closer attention to the sharper dication energy surfaces rather than the flattened monocation surfaces. For the remainder of this paper, we will consider only the dication surface. By considering such pictures we pay closer attention to the frontier orbital terms rather than the interatomic repulsion. By doing so we take into account the fact that, in a μ_2-Hückel calculation, one does not include the attractive portion of the van der Waals forces. Lessening the contribution of the van der Waals repulsion helps compensate for this absence.

3.1.2. Fluoranthene Cation. We apply the same methodology to the fluoranthene cation. Here again only one single-crystal structure is known with short C···C distances, $(\text{fluoranthene})_2PF_6$.[33] Another structure revealed by CSD, $(\text{fluoranthene})_2AsF_6$, was determined at low temperature (120 K) where a slight distortion in the structure due to low-temperature phase transition was observed.[33,86] The structure of $(\text{fluoranthene})_2PF_6$ is illustrated in Figure 9. As this figure shows, the fluoranthene molecules appear as stacks, with neighboring molecules in the stacks being related to each other by inversion centers. There are six closest contacts between neighboring molecules. Neighboring 6a and 10b sites are at 3.24 Å of each other. (See Figure 6 for atomic numbering scheme.) Also the 3 and 4 sites lie directly next to the 7 and 10 sites of the adjoining

(86) Enkelmann, V.; Göckelmann, K. *Ber. Bunsen-Ges. Phys. Chem.* **1987**, *91*, 950−957.

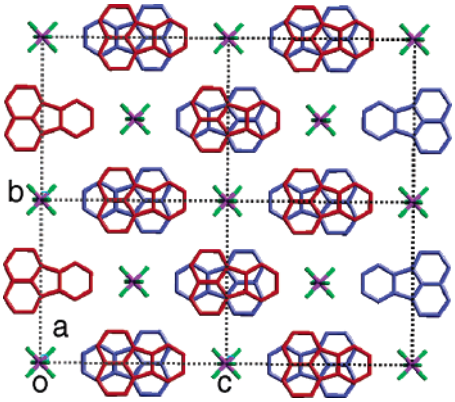

Figure 9. Crystal structure of $(\text{fluoranthene})_2PF_6$. C, red and blue; P, purple; F, green. The two stacked fluoranthene moieties are rotated 180° with respect to one another.

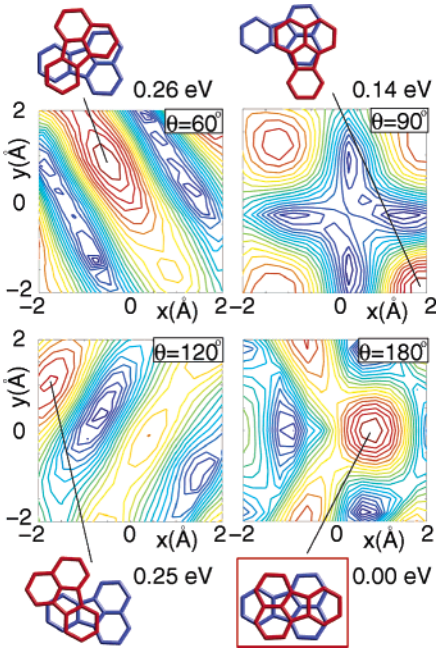

Figure 10. Contour maps of μ_2-Hückel calculations showing the variation of energy of the $(\text{fluoranthene})_2^{2+}$ dimer with respect to its geometry. The global energy minimum geometry is pictured in red box.

fluoranthene molecule at distances ranging from 3.14 to 3.26 Å.

In Figure 10, we plot the μ_2-Hückel energy surface for a dimer of fluoranthene cations with respect to the center-of-mass variables x and y and the orientational variable θ (a picture showing these parameters for fluoranthene is given in the Supporting Information). Figure 10 presents contour plots for four different θ values: 0°, 90°, 120°, and 180°. There are numerous minima on these energy surfaces. The geometries of the four lowest are illustrated in this figure. The global minimum is at $(x, y) = (0.8, 0)$ and $\theta = 180°$. This global minimum is precisely the geometry observed in the $(\text{fluoranthene})_2PF_6$ crystal structure.

The global minimum can be understood through application of the maximin principle. In Figure 6, we show the HOMO of the fluroanthene molecule at both the Hückel and RHF/6-31G(d) levels. As this figure shows, the dominant atomic contributions are at the 3, 4, 6a, 7, 10, and 10b positions. Smaller contributions are found at the 1, 2, 5, 6, 8, and 9 positions. At the 3a, 3b, 6b,

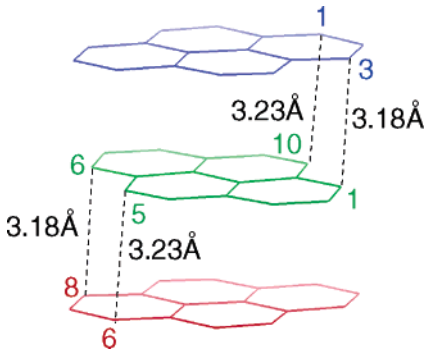

Figure 11. Triple-decker stack illustration in $(pyrene)_{10}(I_3)_4(I_2)_{10}$ crystal structure.

and 10a positions, there is essentially no atomic orbital presence. Applying the maximin principle we therefore wish to maximize contacts between the first 6 sites while simultaneously minimizing contacts with the remaining 10 sites. It is geometrically straightforward to see that the observed inverted geometry maximizes the former contacts while minimizing the latter contacts.

3.1.3. Pyrene Cation. Although there are no pyrene cations with short C···C contacts listed in the CSD, we have recently prepared such a species.[34] Its chemical formula is $(pyrene)_{10}(I_3)_4(I_2)_{10}$. The structure is a complex one with eight crystallographically inequivalent pyrene molecules in the crystal structure. However, if we restrict our attention to those pyrene molecules with C···C contacts of less than 3.25 Å, the crystal structure can be substantially simplified. All short pyrene contacts occur in triple-decker stacks of three face-to-face pyrene molecules. One of these triple stacks is illustrated in Figure 11 (there are two such stacks in the unit cell: they are crystallographically inequivalent).

As Figure 11 shows, the outer two pyrene molecules are both oriented the same way, while the inner pyrene molecule is rotated 60° with respect to them. Each pyrene molecule has seven carbon atoms in close contact with each of its pyrene neighbors. However not all of these seven contacts are at the same short distance. In the example of Figure 11, contact lengths range from 3.16 to 3.37 Å. The former length is considerably shorter than the sum of the van der Waals radii, while the latter is not. This variation in contact distance is due to a slight tilt in the central pyrene molecule.

If we restrict our attention to C···C contacts less than 3.23 Å, there are only two contacts between neighboring pyrene molecules. The 1 and 3 sites of the topmost pyrene molecule are in contact, respectively, with the 10 and 1 site of the middle pyrene molecule, while the 6 and 8 sites of the bottom-most pyrene molecule are, respectively, near the 5 and 6 sites of the middle pyrene molecule. Thus the two ends of the middle pyrene molecule are in contact with different outer pyrene molecules, giving the triple-decker, something of the form of the letter Z. These short contacts range from 3.16 to 3.23 Å.

We can qualtitatively understand this triple decker configuration through the maximin principle. In Figure 6, we show the HOMO of pyrene at both the Hückel and RHF/6-31G(d) levels. As this figure shows, the largest contributions to the HOMO come from the 1, 3, 6 and 8 positions on the pyrene molecule. Slightly smaller contributions are found at the 4, 5, 9, and 10 positions. Unlike the naphthalene and fluoranthene cases, it is impossible to find a stacking arrangement which has contact between the 1, 3, 6, and 8 positions with the centers of mass of the adjacent pyrene molecules near to each other.

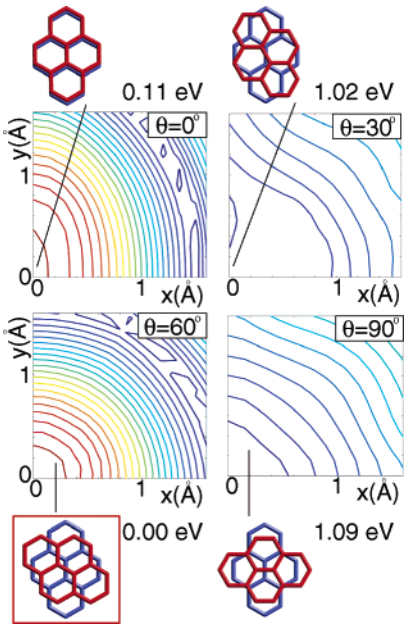

Figure 12. Contour maps of μ_2-Hückel calculations showing the variation of energy of the $(pyrene)_2^{2+}$ dimer with respect to its geometry. The global energy minimum geometry is boxed.

The observed crystal packing has found a remarkable alternate solution by using a triple-decker arrangement. Two of the 1, 3, 6, and 8 sites of the outer pyrene molecule are in close contact with 1, 5, 6, and 10 sites of its pyrene neighbor. Of the four contacts involving the central pyrene molecule, two involve the 1, 3, 6, and 8 sites and two involve the 4, 5, 9, and 10 positions. As the former positions have larger HOMO coefficients than the latter positions, contacts involving the former atoms are shorter than those involving the latter (3.16−3.18 Å vs 3.18−3.23 Å)

The preferred orientation can also be seen in direct calculations on pyrene cation dimer systems. In Figure 12, we show contour maps of two face-to-face pyrene molecules. The three parameters used in these contour plots are x, y, and θ. As in the case of naphthalene, the x and y parameters refer to the translational shift of the center-of-mass of the adjacent molecules (we assume the pyrene molecular plane is strictly normal to the z-axis), while the θ angle refers to the orientation of one molecule with respect to the other. (a figure illustrating these parameters is given in the Supporting Information)

The surfaces shown in Figure 12 have a number of minima. The global minimum is found at x, y, and θ equal to respectively 0°, 0°, and 60°. This relative orientation bears features in common with the observed experimental structure. An examination of Figure 11 shows that any pair of neighboring pyrene molecules in the triple-decker sandwich involve two pyrene molecules where the relative orientation of the neighbors has a θ value of 60°. The 60° dimer packing therefore optimizes the dimer cation surface. (But as we noted above in the experimental structure, this dimer configuration is then placed in a larger trimer piece to further maximize HOMO overlap while minimizing C···C contacts.)

3.2. Oxidized N-Containing π-Radicals: Pc and Pp. In this section, we apply the maximin principle to oxidized N-

containing π-radicals with C···C, C···N, and N···N contacts approximately 5% less than the sums of the van der Waals radii (C···C, 3.20 Å; C···N, 3.09 Å; and N···N, 2.95 Å). Our CSD survey shows that such systems are limited to the well-known macrocycles Pc and Pp. In all the CSD examples, the Pc or Pp configurations involve a face-to-face arrangement.[35−41] As model quantum calculations would require assessing not just C···C but C···N intermolecular contacts, and as ionicity might play a significant role, we do not feel that the μ_2-Hückel Hamiltonian would be useful in an unadapted form. In this section, we therefore focus on the qualitative ability of the maximin principle to rationalize observed Pc and Pp crystal structures.

Interest in oxidized phthalocyanine molecules stems from their conducting properties.[36,87−92] Here the Pc and Pp rings are oxidized radicals with Pc and Pp charges ranging from +0.33 to +1. C···C contacts between rings can be quite short-ranged, as short as 3.16 Å.[93] To understand these short contact distances, we examine the frontier orbitals. The HOMOs (which in these systems are partially filled) are pictured in Figure 13. The 2HPc, MPc, and MPp HOMOs are qualitatively similar. The atoms with the highest contribution to the HOMO come from the carbon atoms of the inner 16-atom ring. There are eight such carbon atoms (the so-called 5, 7, 12, 14, 19, 21, 26, and 28 positions), arranged in an octagonal pattern around the ring center. The phase of these eight sites alternates as one progresses around the ring. By contrast, the eight nitrogen sites of the central 16-atom ring have either zero or rather small contributions.

Applying the maximin principle, we therefore expect the eight central carbon atoms to be in contact with one another while the other atoms to stay away from each other. This is in agreement with the known experimental determinations.[35−39,94,95] Our CSD search, together with the additional crystal structures reported in this paper, reveals that there are fourteen crystal structures with short C···C, C···N, or N···N contacts. All have essentially the same intermolecular orientation (two 2HPc structures, 10 MPc structures, and two MPp structures). This orientation is called the X-form; see Figure 13. It consists of two macrocycles, one directly above the other but rotated about 45° with respect to its neighboring molecule. The two new structures reported in this paper, $(MgPc)(NO_3)_{0.5}THF$ and $(MgPc)(ReO_4)_{1.5}THF$, are further examples of this X-form: the full description of their structures given in the Supporting Information therefore gives complete details on this structure type.

The X-form is an ideal outcome of the maximin principle. The eight atoms which contribute most significantly to the HOMO are in close contact, while the other atoms are not. Furthermore, the phase alternation between the neighboring 5, 7, 12, 14, 19, 21, 26, and 28 positions allows good overlap after the observed 45° rotation. The X-form is therefore the dimer configuration most compatible with the maximin principle.

3.3. Reduced N-Containing π-Radicals: HCCP, TCNQ, DCNQI, BTCQ, TCNE. In the CSD, reduced N-containing π-radicals with short C···C, C···N, or N···N contacts (contact distances < 0.95 the sum of the van der Waals radii, i.e., distances shorter than respectively 3.20, 3.09, and 2.95 Å) all prove to be nitriles. The five nitrile radicals uncovered (HCCP,[42,43] TCNQ,[44−65] DCNQI,[66] BTCQ,[67] and TCNE[68−75]) are shown in Figure 13. All these species are in an open-shell form, with an anionic charge between 0.5 and 1. With one exception[67] these radical anion salts have been obtained by reduction of the neutral species. As these systems are anions, vs the cations of the previous portions of the paper, our attention in this section turns to the partially occupied LUMO. As in the previous section, we wish to demonstrate that the maximin principle based on the partially filled frontier orbital allows us to understand the observed crystal packings.

3.3.1. HCCP. HCCP is a three-fold symmetric planar molecule with a triangle of sp^2 carbon atoms in the center, three exo-carbon positions, and six peripheral nitrile groups. Its LUMO is pictured in Figure 13. This LUMO preserves the three-fold symmetry of the HCCP molecule, with the biggest contribution coming from the three exo-carbon atoms (the 4, 5, and 6 positions). The maximin principle tells us that these atoms will try to establish short contacts to each other, whereas the others will not. It is not geometrically possible to have contacts between all central carbon atoms and no contacts between the remaining atoms.

The observed structure is the optimal one vis-à-vis the maximin principle.[42,43] In the observed packing two of the 4, 5, and 6 positions are superimposed on top of the neighboring molecule, but all other positions are significantly removed from each other. Thus only atoms with the largest LUMO terms are in close contact with each other.

3.3.2. TCNQ and DCNQI. TCNQ is the most widely studied of all nitrile π-radicals. Its LUMO is pictured in Figure 13. The 1, 4, 7, and 8 carbon atoms in this molecule are the sites with the largest contribution to the LUMO. Somewhat smaller coefficients are found on the 2, 3, 5, and 6 carbon positions. There are even smaller contributions from the four nitrile groups. By the maximin principle, the optimal arrangement would involve contact between these four sites and no contact between nitrile groups. Some thought shows that the optimal arrangement would be a face-to-face stacking of two similarly oriented TCNQ molecules in which one TCNQ molecule is displaced along its long axis. In such an arrangement there would be close contacts between three of the four atoms with the largest LUMO presence, and no contact between any other atoms.

The CSD reveals 71 structures with short contacts. All but one have TCNQ molecules in a face-to-face arrangement. In all cases the two neighboring TCNQ molecules have the same orientation. (The lone exception to face-to-face packing has two nitrile moieties of neighboring TCNQ molecules in close contact:[96] a geometry previously analyzed as being due to

(87) Petersen, J. L.; Schramm, C. S.; Stojakovic, D. R.; Hoffman, B. M.; Marks, T. J. *J. Am. Chem. Soc.* **1977**, *99*, 286−288.
(88) Thompson, J. A.; Murata, K.; Miller, D. C.; Stanton, J. L.; Broderick, W. E.; Hoffman, B. M.; Ibers, J. A. *Inorg. Chem.* **1993**, *32*, 3546−3553.
(89) Morimoto, K.; Inabe, T. *J. Mater. Chem.* **1995**, *5*, 1749−1752.
(90) Matsuda, M.; Naito, T.; Inabe, T.; Hanasaki, N.; Tajima, H. *J. Mater. Chem.* **2001**, *11*, 2493−2497.
(91) Inabe, T. *J. Porphyrins Phthalocyanines* **2001**, *5*, 3−12.
(92) Asari, T.; Naito, T.; Inabe, T.; Matsuda, M.; Tajima, H. *Chem. Lett.* **2004**, *33* (2), 128−129.
(93) Palmer, S. M.; Stanton, J. L.; Jaggi, N. K.; Hoffman, B. M.; Ibers, J. A.; Schwartz, L. H. *Inorg. Chem.* **1985**, *24*, 2040−2046.
(94) Martinsen, J.; Pace, L. J.; Phillips, T. E.; Hoffman, B. M.; Ibers, J. A. *J. Am. Chem. Soc.* **1982**, *104*, 83−91.
(95) Yakushi, K.; Sakuda, M.; Hamada, I.; Kuroda, H.; Kawamoto, A.; Tanaka, J.; Sugano, T.; Kinoshita, M. *Synth. Met.* **1987**, *19*, 769−774.
(96) Matsumoto, N.; Nonaka, Y.; Kida, S.; Kawano, S.; Ueda, I. *Inorg. Chim. Acta* **1979**, *37*, 27−36.

Compound (n=1,2)	Neutral Structure[a]	Frontier Orbital Involved (RHF/6–31G(d))	Experimental Packing (CSD search)	CSD Frequency
$(2HPc)_2^{n+}$	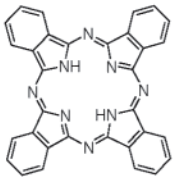		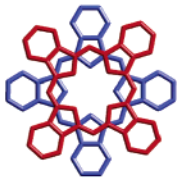	2/2
$(MPc)_2^{n+}$	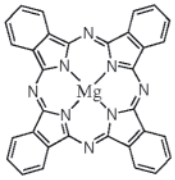		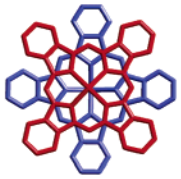	10/10
$(MPp)_2^{n+}$	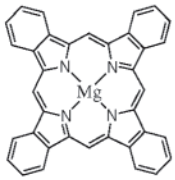	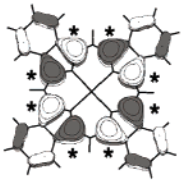	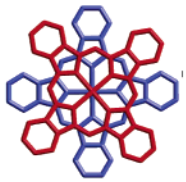	2/2
$(HCCP)_2^{n-}$	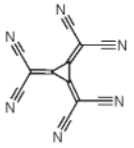	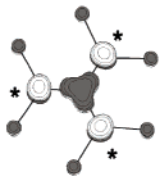	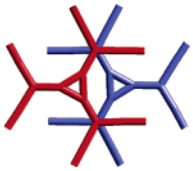	2/2
$(TCNQ)_2^{n-}$	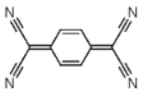	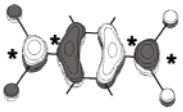		57/71
			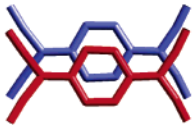	10/71
$(DCNQI)_2^{-}$	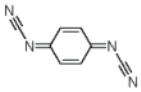			1/1
$(BTCQ)_2^{2-}$	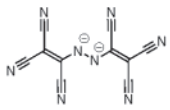		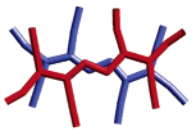	1/1
$(TCNE)_2^{n-}$		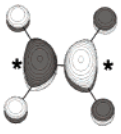		13/13

[a]Except BTCQ

Figure 13. Frontier orbital configurations of nitrile anions and phthalocyanine cations and their corresponding crystal packing geometries and frequencies observed from CSD searches. Stars indicate atoms with the largest frontier orbital contributions.

nitrile−nitrile dipole moment interactions).[97] The two most common of the arrangements of the remaining 70 structures are shown in Figure 13. The most common form (which we term staggered-long axis) has two molecules staggered such that the 1, 4, and 7 positions lie directly above, respectively, the 8, 1 and 4 positions of the molecule beneath. This arrangement is found in 57 of the 71 observed examples.[45,46,48,49,51,52,55,58,62,64,65] This arrangement is the one predicted by the maximin principle.

The second most common arrangement (which we term staggered-short axis) is also shown in Figure 13. In this arrangement the top TCNQ molecule is shifted along the short principal axis of the molecule. In this arrangement the 1, 2, 3, and 4 positions of the top molecule are in closest contact with, respectively, the 6, 1, 4, and 5 positions of the molecule beneath.

(97) Lee, S.; Mallik, A. B.; Fredrickson, D. C. *Cryst. Growth Des.* **2004**, *4*, 279−290.

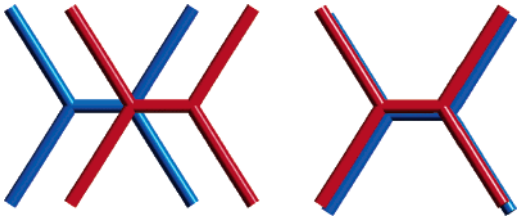

Figure 14. Preferred conformation of TCNE anionic dimer expected by the maximin principle (left) vs the observed TCNE anion π-dimer structure (right).

There are therefore four close contacts in this arrangement, but these close contacts involve atoms with somewhat smaller orbital coefficients. Qualitatively, this appears to us a slightly less ideal intermolecular packing with respect to the maximin principle. This is substantiated by the smaller number of structures (ten) which adopt the staggered-short axis arrangement.[44,47,50,53,54,59,61−63] This second arrangement, as it involves contacts between atoms all with large (although not the largest) HOMO presences, nonetheless seems a reasonable alternative.

In the remaining three structures, each one adopts their own different arrangement. In one case the TCNQ molecules are fully eclipsed, with one molecule directly on top of the other.[56] In the other two cases, the neighboring molecules are fully staggered along the long axis: one of the nitrile groups of one molecule is in contact with the other molecule.[57,60] These remaining three configurations therefore do not follow the maximin principle. Thus the maximin principle helps us understand only the most common intermolecular arrangement, the arrangement which presumably corresponds to the global minimum of the dimer system.

Finally, we consider DCNQI, a molecule highly related to TCNQ. In this molecule there are only two nitrile groups. Its LUMO is nonetheless similar to that of TCNQ; see Figure 13. Following the maximin principle, the expected packing is the staggered-long axis arrangement discussed previously for TCNQ. The single observed structure reported in the CSD confirms this expectation.[66]

3.3.3. BTCQ. The structure of BTCQ is illustrated in Figure 13. Its partially occupied frontier orbital is also shown in this figure. The atoms most involved in the frontier orbital are the peripheral 1 and 6 carbon atoms and the central 3 and 4 nitrogen positions. All other atomic contributions are small. The single known crystal structure accords well with the maximin principle.[67] In this structure each BTCQ molecule is in close contact with two molecules. In the primary neighbor there are four close contacts between BTCQ molecules with a shortest contact distance of 2.82 Å (an N···N contact), while in the secondary neighbor there is only one close contact at 3.00 Å (a C···N contact). The geometry between each BTCQ molecule and its primary neighbor is shown in Figure 13. Its four close contacts all involve the four atoms with large LUMO coefficients. Thus all large orbital coefficient atoms are involved in a close contact and all remaining atoms do not form a close contact, in agreement with the maximin principle.

3.3.4. TCNE. Tetracyanoethene (TCNE) anion radical is the simplest of all the radicals discussed in this paper. The LUMO is predominantly located on the ethylene carbon atoms. By the maximin principle one would expect the preferred conformation to have the staggered-form shown in Figure 14 (left). Instead, as Figure 13 shows, all 13 observed structures have fully eclipsed TCNE dimers.[68−75] (It can be noted that in two of these thirteen eclipsed structures there are also subsidiary short contacts between non-face-to-face TCNE molecules.[98]) (For a complete list of structures, see CSD search results in the Supporting Information.)

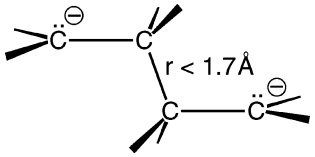

Figure 15. Experimentally observed TCNE dianion structure, also known as the $TCNE^{-}$ σ dimer.

Sufficient work has been carried out on the $(TCNE)_2^{2-}$ system that we are able to rationalize this breakdown of the maximin principle. The maximin principle is a procedure by which to find the global minimum for two face-to-face π-radicals at a fixed plane-to-plane distance. But in the case of $(TCNE)_2^{2-}$ these intermolecular dimers are not themselves stable with respect to the formation of a single dianion molecule. Thus while the geometry expected by the maximin principle is not observed, the dianion illustrated in Figure 15 is known.[99] In other words in the case of the maximin geometry, frontier orbital interactions are so strong that interatomic repulsions are unable to prevent true bond formation. Indeed perhaps the reason that the eclipsed TCNE form is observed is that, in this latter geometry, due to the nitrile contacts, there are greater interatomic repulsion energies, thus stabilizing the intermolecular system.

3.3.5. Summary. Examination of the HCCP, TCNQ, DCNQI, and BTCQ compounds shows that the atoms which contribute most to the partially filled frontier orbital have short contacts between each other, whereas chemical groups with small frontier orbital contributions do not. Nitrile moieties are not sterically bulky, but as they have small frontier orbital presences, they tend to repel each other. Short contacts between nitrile groups are indeed almost never observed. Interestingly, the maximin principle appears to apply equally well to mixed valence systems as non mixed valence systems.

3.4. Predicted Oligoacene Cation Structures. In the preceding sections we have shown that the maximin principle can be used to rationalize known aromatic hydrocarbon and N-containing π-system ion dimer structures. Its success in rationalizing ion dimer structures suggests that this same principle can be used for prediction as well as rationalization. Such predictions could be useful as it is sometimes extremely difficult to synthesize chemically stable π- ion structures.

In this section we consider some larger arene cation radicals, the oligoacenes. Oligoacenes are oligocyclic hydrocarbons consisting of fused benzene rings. Due to their semiconducting properties, these compounds are extensively studied.[100−108] (Pentacene with five fused aromatic rings is currently the organic semiconductor with highest field-effect mobility at room temperature.[109−113])

(98) Miller, J. S.; Glatzhofer, D. T.; Vazquez, C.; Mclean, R. S.; Calabrese, J. C.; Marshall, W. J.; Raebiger, J. W. *Inorg. Chem.* **2001**, *40*, 2058−2064.
(99) Zhang, J.; Liable-Sands, L. M.; Rheingold, A. L.; Sesto, R. E. D.; Gordon, D. C.; Burkhart, B. M.; Miller, J. S. *Chem. Commun.* **1998**, 1385−1386.
(100) Kivelson, S.; Chapman, O. L. *Phys. Rev. B* **1983**, *28*, 7236−7243.
(101) Wiberg, K. B. *J. Org. Chem.* **1997**, *62*, 5720−5727.
(102) Herwig, P. T.; Müllen, K. *Adv. Mater.* **1999**, *11*, 480−483.
(103) Bock, H.; Gharagozloo-Hubmann, K.; Sievert, M.; Prisner, T.; Havlas, Z. *Nature* **2000**, *404*, 267−269.
(104) Houk, K. N.; Lee, P. S.; Nendel, M. *J. Org. Chem.* **2001**, *66*, 5517−5521.

As hole conductors, the implicit cation states are transient in nature. In this paper the focus is on the crystal structure adopted by nontransient holes. Even here our knowledge of cation packing is limited. No crystal structure of any oligoacene cation with more than three fused benzene rings has ever been reported. To confer stability on these larger systems, apparently substantial substituents are needed.[114−119] We therefore can apply the maximin principle to predict the stacking geometry of crystalline oligoacene cations (holes).

In Figure 16, we show the HOMOs of the series of oligoacene systems presented at the Hückel level. As can be seen in this figure, the HOMOs are all structurally similar. The atomic coefficients of all bridged sites are uniformly small. The principal HOMO contributions come from nonfused carbon sites α to bridging positions. These principal contributions are largest toward the center of the molecule, with coefficients of neighboring nonbridging sites (α to the fused positions) of opposite phase to one another.

The structural consequences of this HOMO have been previously discussed for the simplest of all oligoacenes, naphthalene itself. The lowest energy dimer structure, which both maximizes the HOMO−HOMO contact and minimizes the number of interatomic contacts, is the one in which the two molecules are oriented at 90° to each other. Given the similarities between the naphthalene and larger oligoacene HOMOs, it is not surprising that the oligoacene cation dimer global minima generally involve two molecules with such a 90° orientation with respect to each other.

In Figure 17, we show an energy contour map for two hexacene cations rotated 90° with respect to each other. (We have surveyed θ angles over the full range of possible θ values, and the Hückel global minimum proved to be at $\theta = 90°$. We have also calculated the RHF energies at just two geometries: $x = y = 0$, $\theta = 0°$ and $x = y = 0$, $\theta = 90°$. At the RHF 6-311G-(d,p) level, the global minimum predicted by μ_2-Hückel calculatons is decidedly below the eclipsed geometry, by 1.35 eV.) The Hückel contour map at this angle is plotted with respect to two variables, x and y. These variables refer to the lateral translation of the center-of-masses of the two hexacene molecules (we have assumed that the hexacene molecules are perfectly face-to-face to each other at a distance of 3.2 Å and that these planar molecules are normal to the z-direction). As Figure 17 shows, there are a number of local minima in this structure. Each of these local minima occur when carbon atoms α to the bridging sites come into close contact with the adjacent molecule.

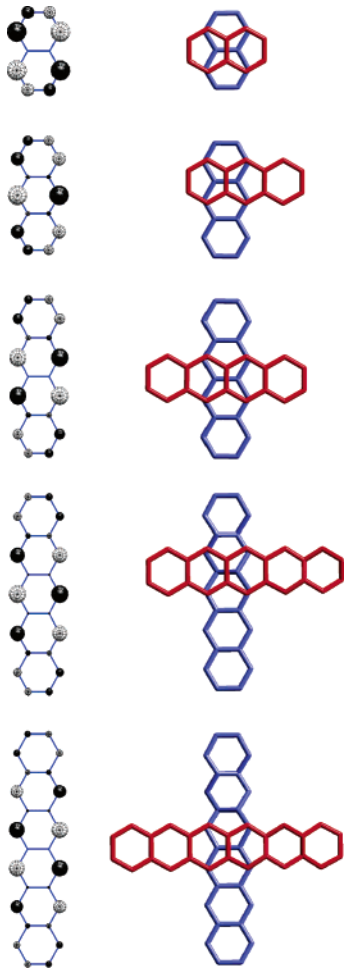

Figure 16. HOMOs of a series of oligoacene cation systems presented at the Hückel level. Their lowest energy stacking geometries at 90° are also shown in the right column.

For all local minima there are only four closest contacts. Differences in energy between these minima are up to 0.42 eV, with those local minima involving more central carbon atoms the lowest in energy. This does not mean, however, that intermolecular interactions involving the most central carbon atoms should be the experimentally favorable geometry. With a molecule of sufficient size, such as hexacene itself, if one has intermolecular contacts involving the more peripheral carbon atoms, it becomes possible to place two hexacene cations above or beneath each other, thus doubling the number of good HOMO−LUMO contacts.

4. Conclusions

It is well-known that structures and reaction pathways are governed by electronic (frontier orbital) and steric (hard-core repulsion) factors. The maximin principle applied in this paper is an embodiment of these two principles. The maximin principle though does tell us something beyond the invocation of electronic and steric factors. It points to a structural transition. When molecules are further apart than the sum of the van der

(105) Anthony, J. E.; Brooks, J. S.; Eaton, D. L.; Parkin, S. R. *J. Am. Chem. Soc.* **2001**, *123*, 9482−9483.
(106) Raghu, C.; Pati, Y. A.; Ramasesha, S. *Phys. Rev. B* **2002**, *65*, 155204.
(107) Karl, N. *Synth. Met.* **2003**, *133*−*134*, 649−657.
(108) Bendikov, M.; Duong, H. M.; Starkey, K.; Houk, K. N.; Carter, E. A.; Wudl, F. *J. Am. Chem. Soc.* **2004**, *126*, 7416−7417.
(109) Lin, Y.-Y.; Gundlach, D. J.; Nelson, S. F.; Jackson, T. N. *IEEE Electron Device Lett.* **1997**, *18*, 606−608.
(110) Dimitrakopoulos, C. D.; Malenfant, P. R. L. *Adv. Mater.* **2002**, *14*, 99−117.
(111) Jurchescu, O. D.; Baas, J.; Palstra, T. T. M. *Appl. Phys. Lett.* **2004**, *84*, 3061−3063.
(112) Thorsmølle, V. K.; Averitt, R. D.; Chi, X.; Hilton, D. J.; Smith, D. L.; Ramirez, A. P.; Taylor, A. J. *Appl. Phys. Lett.* **2004**, *84*, 891−893.
(113) Deng, W.-Q.; Goddard, W. A., III. *J. Phys. Chem. B* **2004**, *108*, 8614−8621.
(114) Buravov, L. I.; Zvereva, G. I.; Kaminskii, V. F.; Rosenberg, L. P.; Khidekel, M. L.; Shibaeva, R. P.; Shchegolev, I. F.; Yagubskii, E. B. *J. Chem. Soc., Chem. Commun.* **1976**, 720−721.
(115) Kato, R.; Kobayashi, H.; Kobayashi, A. *Physica* **1986**, *143B*, 304−306.
(116) Inabe, T.; Mitsuhashi, T.; Maruyama, Y. *Bull. Chem. Soc. Jpn.* **1988**, *61*, 4215−4224.
(117) Chetcuti, P. A.; Hofherr, W.; Liégard, A.; Rihs, G.; Rist, G.; Keller, H.; Zech, D. *Organometallics* **1995**, *14*, 666−675.
(118) Kochi, J. K.; Rathore, R.; Le Maguères, P. *J. Org. Chem.* **2000**, *65*, 6826−6836.
(119) Sekizaki, S.; Tada, C.; Yamochi, H.; Saito, G. *J. Mater. Chem.* **2001**, *11*, 2293−2302.

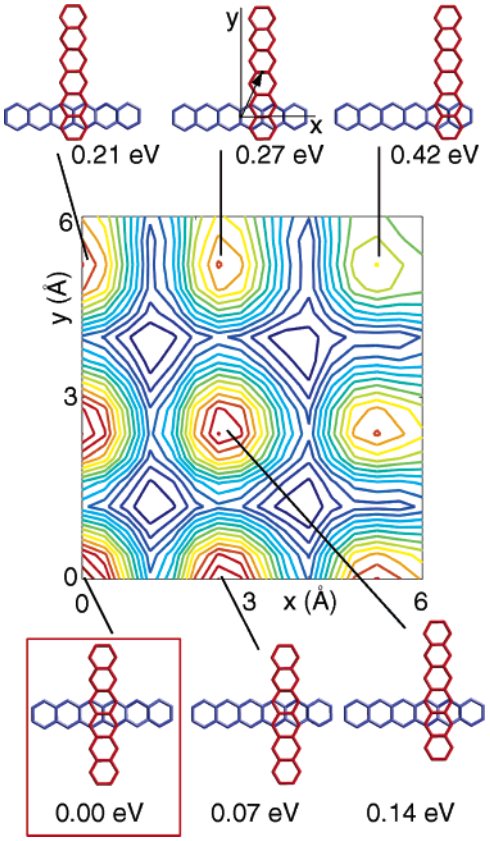

Figure 17. Contour maps of μ_2-Hückel calculations showing the variation of energy of the $(\text{hexacene})_2^{2+}$ dimer with respect to its geometry. The global minimum geometry is boxed.

Waals radii of their constituent atoms, both the van der Waals and frontier orbital interactions have significant attractive components; one cannot reduce each of these terms to mere attractive or repulsive roles; and the maximin principle can break down. The maximin principle is therefore clearest when intermolecular contacts are 5% less than the sum of the constituent atoms' van der Waals radii.

The maximin principle goes hand-in-hand with the role of the sum of van der Waals radii as a critical parameter. As the atoms of neighboring molecules come closer than the sum of their van der Waals radii, and as these van der Waals interactions become increasingly repulsive, one turns increasingly to the maximin situation. Indeed, for the structures discussed in this paper, which all involve dimers near the onset of the repulsive van der Waals regime, there are still substantial attractive van der Waals terms. These attractions presumably play a role in bringing the centers-of-mass of neighboring molecules close to each other, an effect which has been seen throughout this paper.

Second, our numerical studies involving the μ_2-Hückel Hamiltonian suggest a simple way in which steric repulsions can be incorporated into the Hückel formalism. The accuracy of this approximation has been tested by comparison with ab initio theory. Traditionally, such repulsions arise from the extended Hückel approximation where repulsive energies come from the filled antibonding orbitals being more antibonding than filled bonding orbitals being bonding. Here we use an alternate tactic, where repulsion comes not from occupation of the antibonding terms but from the trace of the square of the Hamiltonian, a quantity independent of the number of filled antibonding orbitals. This latter term is chosen as this trace is proportional to coordination number. As repulsive interactions are short-range, a linear relation between repulsive energy and the number of contacts seems reasonable. It would be of interest, to adapt this Hamiltonian to either the N-containing π-radicals discussed in this paper or more ambitiously to sulfur systems (which may contain new terms due to the third row sulfur atoms) or fluorinated hydrocarbons (which may contain substantial ionic terms).

Acknowledgment. We are grateful for the financial support of the National Science Foundation (through Grant DMR-0104267 and CHE-0209934). T.D. thanks the French Minister of the Foreign Affairs for a Lavoisier grant. We thank Professor John Marohn for useful discussions.

Supporting Information Available: Canonical ring numbering, CSD search results for π-hydrocarbon and N-containing π-radicals, Crystallographic data and structural descriptions of the two magnesium phthalocyanine radical salts (**1** and **2**), and TCNQ radical anion packings. Complete author list of reference 82. Figures illustrating the x, y, and θ parameters for fluoranthene and pyrene. This material is available free of charge via the Internet at http://pubs.acs.org.

JA050346F